Optimization of the Dynamic Response of a Complete Exhaust System

T. Lauwagie, J. Strobbe, E. Dascotte
Dynamic Design Solutions
Interleuvenlaan 64, B-3001, Leuven, Belgium
email: **tom.lauwagie@dds.be**

J. Clavier, M. Monteagudo
Faurecia Exhaust System Division – R&D Center
Bois sur Prés, 25550, Bavans, France
email: **josiane.clavier@faurecia.com**; **mauricio.monteagudo@faurecia.com**

Abstract
This paper presents an optimization approach for tailoring the dynamic response of a complete exhaust system using finite element modeling. Before the optimization procedure is started, the FE-model is updated using modal test data. This preliminary step is required to ensure the validity of the initial FE-model. The actual optimization routine consists of two iteration loops: an inner and an outer loop. The inner iteration loop performs the optimization using a modal domain modification technique to predict the change of the dynamic response of the structure. In this way the structure can be optimized in a computational efficient way. However, the modal domain prediction is only accurate within a limited parameter range. Therefore, the outer iteration loop re-evaluates the full finite element model once the parameter changes exceed the 'trust-region' bounds of the modal domain prediction. The solution of the re-evaluation is then used as improved base for the modal domain prediction in the inner iteration loop.

The suggested optimization approach is illustrated on a finite element model of an exhaust system of a passenger car. The exhaust system is connected to the car body using four isolators. The optimization is performed to keep the force transmitted by the exhaust system through the isolators to the car body below the design specifications, optimizing the stiffness of the decoupling elements. The goal is to ensure a good NVH (Noise Vibration Harshness) performance of the exhaust system.

1 Introduction

Automotive industry requirements for quality, productivity and cost efficiency are at a level where optimization of the design and manufacturing of a product must occur in the earliest stages of conception. The time spent in trial and error analysis in the design process needs to be eliminated for a manufacturer to remain competitive in a global market.

The finite element optimization approach allows an efficient evaluation of designs using advance mathematical tools. Methods must be developed, however, to create fully parameterized models for optimization which can be experimentally verified under pertinent loading conditions.

Exhaust systems present a special case for parameterization because of their geometry and the constraints placed on their design by the underbody of the car. In order to create a model that allows an optimization algorithm to find the "best" feasible design, special care must be taken to limit the parameters defined in the problem. The objective of this study was to develop and verify a procedure for the optimization of the dynamic response of a complete exhaust system.

Exhaust systems are submitted to many dynamic input loads, the most important one coming from the engine. The induced vibrations are spread along the exhaust system, and forces are transmitted to the car

body through the attached points. To reduce the force levels, decoupling elements like ball-joints or flex-couplings (to reduce the engine vibration level transmitted to the exhaust system), and isolators (to reduce the vibrations transmitted to the car body – hanging force) are used. As these vibrations could induce structural borne noise in the passenger compartment, it is necessary to define the best decoupling elements that allow reduce their amplitude to meet their target values.

The behavior of the exhaust system under engine load is simulated using a commercial FEM solver and the correlation with experimental data, model updating, and optimization are done using the FEMtools software [1]. The goal of the correlation and updating is to ensure the representativeness of the FE-model, while the target of the optimization is to define the optimal design parameters in order to reach the specified targets.

This paper presents the collaboration carried out between Faurecia Exhaust System Division & Dynamic Design Solutions. After a short description of the exhaust system used as a reference, the correlation loop will be described. Next, the harmonic response (dynamic behavior) of the exhaust system under engine load will be introduced. Finally, the optimization loop will be addressed.

2 The Exhaust System

2.1 System Description

An exhaust system is made up of pipes, acoustic and emission control components and decoupling elements. The pipe path, the location and size of the volumes are defined according the performances in each domain to be reached and the place available under the car body.

The exhaust system used in this paper has a ball-joint at the inlet pipe, two acoustic volumes and is hanged using four isolators. The front ones and the rear ones are similar in pairs. The location of hangers is a compromise among considering :

- Natural deformed shapes of the exhaust system.
- Balance distribution of static force.
- Packaging area available under the car body.

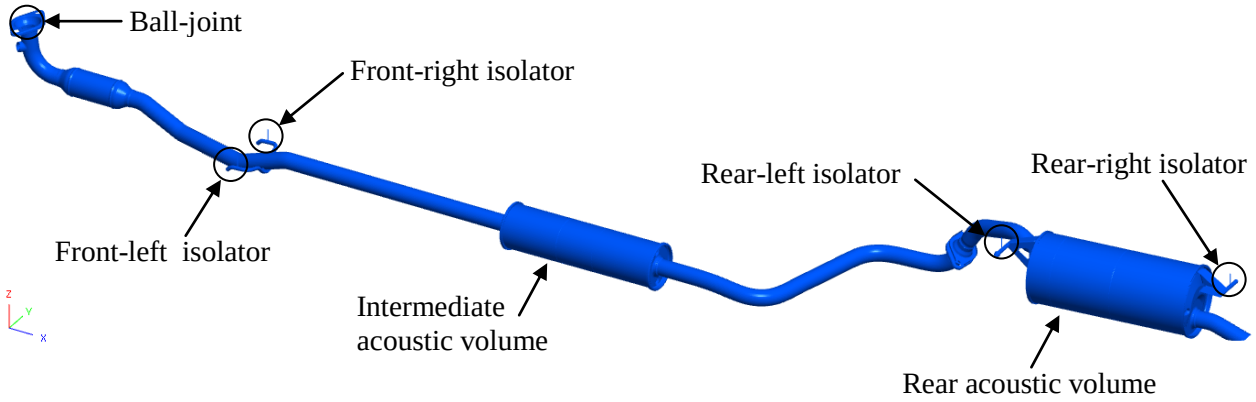

Figure 1: Exhaust system description.

The FE-model of the considered exhaust system consists of 107156 elements (mainly quad4) and has 646200 degrees of freedom.

2.2 Model Updating

Before working on the exhaust optimization, it is necessary to ensure the representativeness of the FE-model. This is done by performing a modal-based correlation, i.e. the comparison between a simulated and an experimental modal basis [2].

The basic principle of the correlation is described in the Figure 2. The FE-model takes into account the geometry of the tested exhaust system and nominal values for size, thickness, material properties, etc. The correlation start once the experimental modal analysis is done. Then, the updating loops are launched.

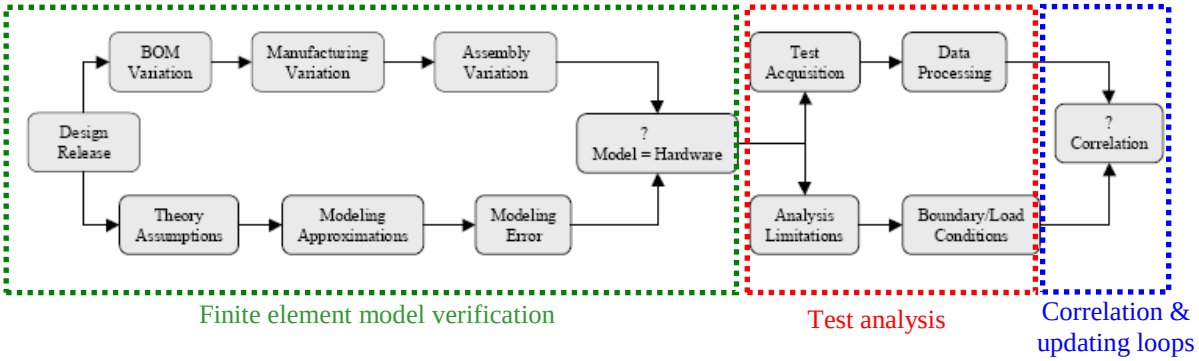

Figure 2: Flow chart of the correlation loop.

2.2.1 Test Set-up and Results

The exhaust system under study was installed on a dynamic test bench in a similar way as it would be in operational conditions, The test set-up is shown in the picture 1.

Picture 1: Exhaust system fixed on the test bench.

The location of the measurement points is defined directly on the exhaust system in order to ensure the representativeness of the test geometry using a 3D metrology tool. (Figure 3).

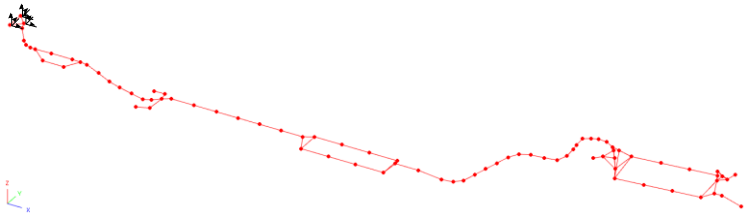

Figure 3: The measurement and loading points.

The acquisition of experimental data was carried out using a shaker to induce forces into the exhaust system. The location of the loading point was defined in such way that all the eigenmodes of the structure in the frequency range of interest were excited. Tri-axial accelerometers were used to obtain all three DOFs in every point of the mode shapes. The experimental modal basis in operational conditions is extracted from FRF measurements (table 1).

Mode	Frequency	Damping	Mode	Frequency	Damping
1	11.60	2.93%	13	181.88	0.73%
2	18.14	3.43%	14	218.71	0.50%
3	22.14	0.99%	15	266.71	0.57%
4	25.53	1.53%	16	283.25	0.50%
5	42.52	1.19%	17	312.23	1.14%
6	45.50	0.94%	18	335.11	0.37%
7	65.85	0.76%	19	340.29	0.66%
8	75.77	0.65%	20	346.45	0.79%
9	97.40	0.54%	21	360.42	0.55%
10	114.28	0.34%	22	366.17	0.92%
11	129.24	0.13%	23	392.71	0.78%
12	148.33	0.29%	24	409.55	1.66%

Table 1: Experimental modal basis.

2.2.2 Modal Basis Correlation in Operational Conditions

The simulated and experimental modal basis are compared using the FEMtools correlation module. To compute the Modal Assurance Criterion (MAC), equation (1) is used:

$$MAC(\psi_a,\psi_e)=\frac{\left|\left(\{\psi_a\}^t\{\psi_e\}\right)\right|^2}{\left(\{\psi_a\}^t\{\psi_a\}\right)\left(\{\psi_e\}^t\{\psi_e\}\right)} \quad (1)$$

where ψ_a represents an analytical mode shape and ψ_e represent an experimental mode shape.

In the considered case, an initial correlation provided encouraging results. The analytical (FEA) and experimental (EMA) modal basis were relatively close. The MAC values indicate a good correlation, only some frequency deviations (the first two modes) were too significant (table 2).

Pair	FEA [Hz]	EMA [Hz]	Diff. [%]	MAC [%]	Pair	FEA [Hz]	EMA [Hz]	Diff. [%]	MAC [%]
1	9.73	11.60	-16.15	94.9	11	130.96	129.24	1.33	97.3
2	14.94	18.14	-17.64	92.2	12	152.97	148.33	3.13	97.3
3	21.76	22.14	-1.69	98.4	13	189.37	181.88	4.12	97.6
4	24.29	25.53	-4.83	94.9	14	229.18	218.71	4.78	95.4
5	41.77	42.52	-1.75	87.3	15	282.68	266.71	5.99	81.2
6	44.69	45.50	-1.79	74.5	16	293.82	283.25	3.73	93.6
7	65.44	65.85	-0.63	97.6	17	324.46	312.23	3.92	91.0
8	77.57	75.77	2.38	97.3	18	346.54	335.11	3.41	84.3
9	96.43	97.40	-1.00	97.0	19	365.21	360.42	1.33	86.5
10	116.67	114.28	2.09	98.0					

Table 2: Analytical and experimental modal basis correlation before updating.

The FE-model had to be updated in order to improve the correlation results by minimizing the frequency deviation and maximizing the MAC values. Updating was performed using the FEMtools updating module.

2.2.3 Updating Loop

In this step, it is necessary to first identify the parameters of the FE-model to be adjusted and the target values (responses) to be reached. In a general case, parameters could be any characteristic or property of the model (thickness, material properties …) and of course, the characteristics of the decoupling elements. The experimental modal data was selected as targets to reach.

A primary step of this study, which is not described in this text, was to check the representativeness of the FE model of the exhaust system itself (i.e. without ball-joint and isolators). The decoupling elements used to attach the complete exhaust system on the test bench were later added to the model as spring elements with 3 DOFs for each isolator and 6 DOFs for the ball-joint.

The behavior of these components under pre-load was not considered. That means that only their nominal parameter value could be tuned in order to improve the modal basis correlation. The updating focused on the characteristics of the ball-joint and isolators. Applying the model updating flow chart (Figure 3), the modal basis correlation was improved with the results shown in table 3.

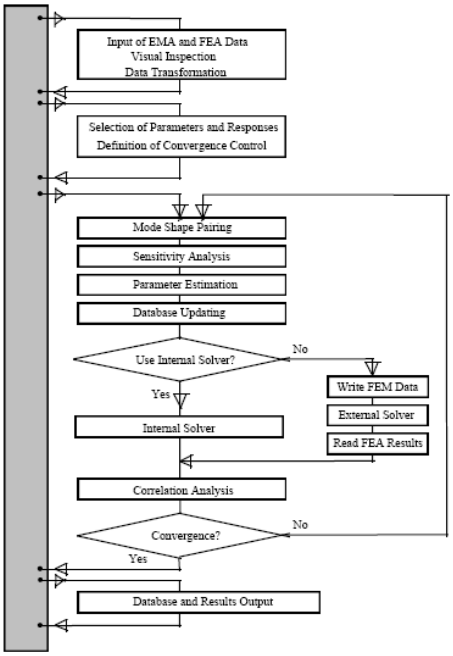

Figure 3: Model updating flow chart.

Pair	FEA [Hz]	EMA [Hz]	Diff. [%]	MAC [%]	Pair	FEA [Hz]	EMA [Hz]	Diff. [%]	MAC [%]
1	11.59	11.60	-0.13	96.8	11	130.64	129.24	1.08	97.2
2	18.08	18.14	-0.35	93.7	12	152.46	148.33	2.78	96.0
3	21.54	22.14	-2.72	97.7	13	184.25	181.88	1.30	96.4
4	25.13	25.53	-1.56	94.9	14	223.44	218.71	2.16	95.3
5	42.69	42.52	0.41	98.4	15	277.47	266.71	4.04	80.3
6	44.66	45.50	-1.85	93.6	16	291.62	283.25	2.96	93.6
7	66.28	65.85	0.65	97.8	17	320.93	312.23	2.78	89.8
8	77.11	75.77	1.78	96.8	18	341.87	335.11	2.02	82.4
9	94.54	97.40	-2.93	94.9	19	362.31	360.42	0.52	86.8
10	115.55	114.28	1.11	97.4					

Table 3: Analytical and experimental modal basis correlation after updating.

The target of the updating loop was reached as it has been shown that the FE-model of the exhaust system is capable of sufficiently reproducing the experimental frequencies and shapes, only by changing the parameter values of the decoupling elements. This implies that the representativeness of the FE-model of the actual exhaust system (the system without the decoupling elements) is ensured, and that the FE-model can be used to optimize the parameter values of the decoupling elements.

3 Response Computation

3.1 Harmonic Response Computation

3.1.1 Theory

The goal of the harmonic response computation is to compute the force transmitted through the isolators to the car body as a function of frequency. The computation of the responses using a direct method is too slow to be used for optimization purposes. Therefore, the harmonic responses are computed using a modal-based approach [3-4].

The modal-based computation of the forced responses starts with the computation of the modal stiffness matrix $[K_m]$, the modal damping matrices $[B_m]$ (structural damping) and $[C_m]$ (modal and viscous damping), and the modal mass matrix $[M_m]$.

$$\begin{aligned}[K_m] &= [\Psi]^T [K][\Psi] \\ [B_m] &= [\Psi]^T [B][\Psi] \\ [C_m] &= [\Psi]^T [C][\Psi] \\ [M_m] &= [\Psi]^T [M][\Psi]\end{aligned} \tag{2}$$

For every frequency $\omega = 2\pi f$, the dynamic modal stiffness matrix can be computed as

$$[D(\omega)] = \left([K_m] - \omega^2 [M_m]\right) + \left([C_m] + \omega [B_m]\right) i \tag{3}$$

The modal load vector $\{p(\omega)\}$ is computed from the harmonic load vector $\{F(\omega)\}$ as

$$\{p(\omega)\} = [\Psi]\{F(\omega)\} \tag{4}$$

Using the dynamic modal stiffness matrix and the modal load vector, the modal displacement vector $\{q(\omega)\}$ can by computed by

$$\{q(\omega)\} = [D(\omega)]^{-1}\{p(\omega)\} \tag{5}$$

The displacement of the two nodes of a spring element that models a isolator is obtained by transformation of the modal displacements to the spatial domain.

$$\begin{aligned}u_{a,x}(\omega) &= \langle \Psi_{a,x} \rangle \{q(\omega)\} \\ u_{b,x}(\omega) &= \langle \Psi_{b,x} \rangle \{q(\omega)\}\end{aligned} \tag{6}$$

in which $u_{a,x}$ and $u_{b,x}$ are the displacement of the first and second node of spring in the local x direction of the considered spring. The matrix rows $\langle \Psi_{a,x} \rangle$ and $\langle \Psi_{b,x} \rangle$ are the mode shape vector components in the local x direction of the first and second node of the spring element. The harmonic response, i.e. the force in the spring element, can be computed from the spring stiffness as:

$$HR_i(\omega) = \left(u_{b,x}(\omega) - u_{a,x}(\omega)\right) k_{i,x} \tag{7}$$

Once the resonant frequencies and mode shapes of the structure are known, the harmonic responses of the isolator forces are computed by evaluating expression (3) to (5) for every frequency line, and expressions (6) and (7) for every isolator.

3.1.2 Application

The engine behavior is mainly defined by the displacement of the piston along its axis. For that reason; as a first approach, only this component could be taken into account to compute the exhaust system response.

In our case study, acceleration measurements were carried out on the exhaust system fixed on the car in run up conditions. Acceleration data at the inlet of the exhaust system – Figure 4 – were used as input load for the dynamic simulations.

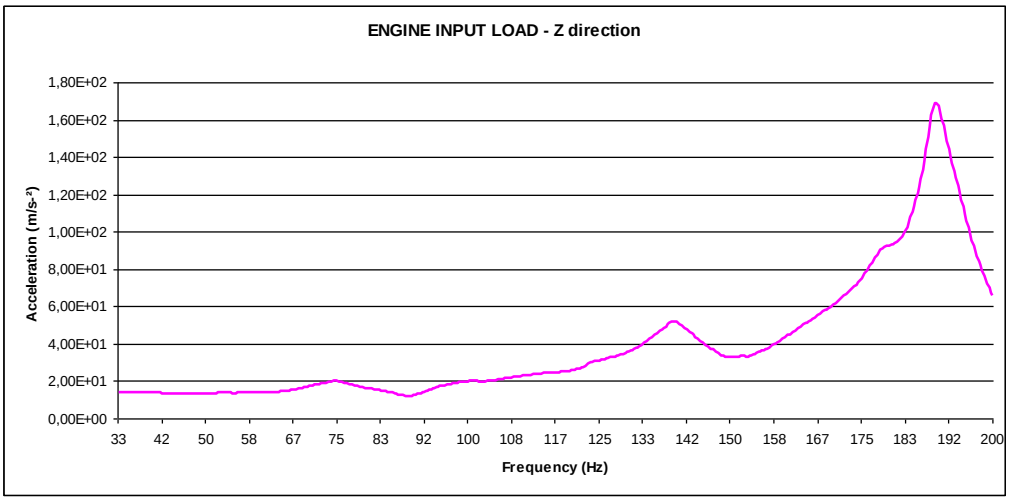

Figure 4: Engine input load.

The amplitude values of the hanging forces are very sensitive to the damping assumptions. For this reason experimental modal damping values were used to model the damping of the exhaust system; structural damping was used to model the damping in the hangers and ball-joint. The vertical hanging force values computed under the above assumptions are given in Figure 5. Note that the forces transmitted in the *Z*-direction exceed the acceptance criterion level, and this for all four isolators.

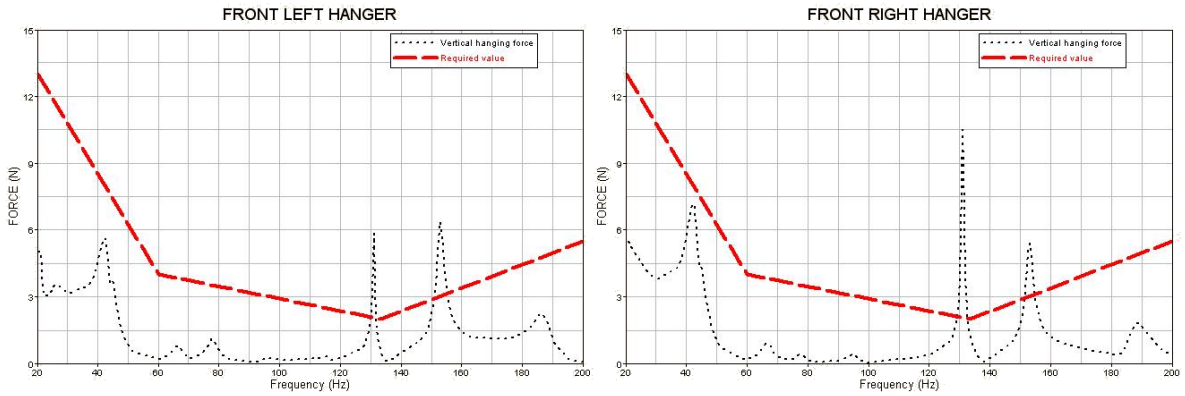

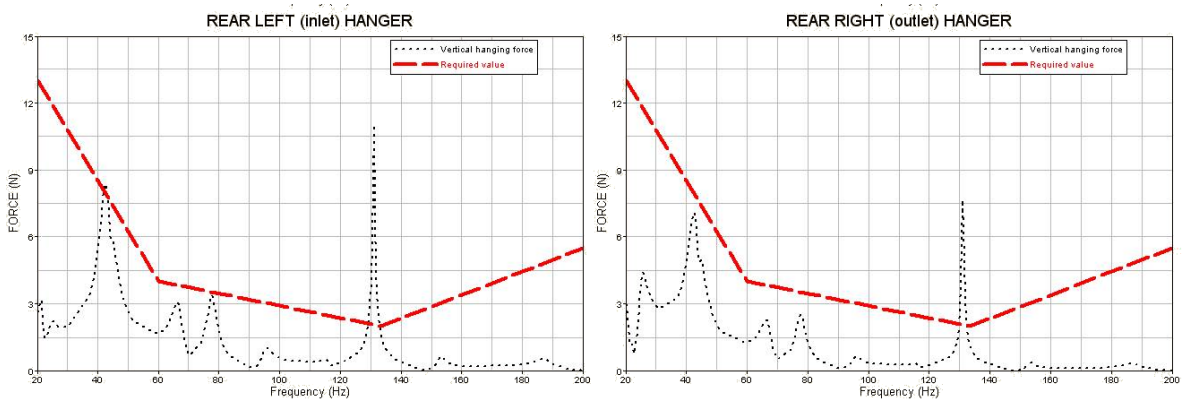

Figure 5: Hanging forces under engine load. The transmitted forces (black) compared to the design specifications (red) in the local *Z*-direction.

3.2 Harmonic Response Modification

The harmonic responses of a modified model can be obtained by computing the resonant frequencies and modes shapes of the modified structure, and using these new frequencies and mode shapes in the equations (2) to (7). The main disadvantage of this approach is that every modification requires an additional run of the FE-solver to compute the frequencies and mode shapes.

The modal-based harmonic response computation allows an alternative approach to estimate the impact of a modification of the system on the harmonic responses. Instead of re-computing the mode shape vectors, the initial vectors are used to compute the effect of the modification on the model stiffness, damping and mass matrices.

$$\begin{aligned} [\Delta K_m] &= \sum_{i=1}^{n_p} \left([\Psi_e]^T \left([K_e(p_i + \Delta p_i)] - [K_e(p_i)] \right) [\Psi_e] \right) \\ &\vdots \\ [\Delta M_m] &= \sum_{i=1}^{n_p} \left([\Psi_e]^T \left([M_e(p_i + \Delta p_i)] - [M_e(p_i)] \right) [\Psi_e] \right) \end{aligned} \tag{8}$$

in which n_p is the number of modified model parameters, p_i is the initial value of the i^{th} parameter, Δp_i is the modification of the i^{th} parameter, $[\Psi_e]$ is the shape vector matrix reduced to the DOFs of element e, and $[K_e]$ is the element stiffness matrix.

Based on the results of expression (8), the modal matrices of the modified system can be estimated.

$$\begin{aligned} [K_m^{\text{mod}}] &= [K_m] + [\Delta K_m] \\ [B_m^{\text{mod}}] &= [B_m] + [\Delta B_m] \\ [C_m^{\text{mod}}] &= [C_m] + [\Delta C_m] \\ [M_m^{\text{mod}}] &= [M_m] + [\Delta M_m] \end{aligned} \tag{9}$$

The harmonic responses of the modified system can now be approximated by inserting the modal matrices of the modified system (9) into expression (3) to (7).

The modal-based prediction of the effect of a modification of a model parameter on the transmitted forces appears to be very reliable, even for relatively large parameter modifications. Consider a reduction of the vertical stiffness of the front-left isolator with 25%. Figure 6 compares the transmitted force obtained using re-analysis with the transmitted force obtained using the modal-based prediction. The maximal offset between the amplitude of the two considered responses is less than 1%.

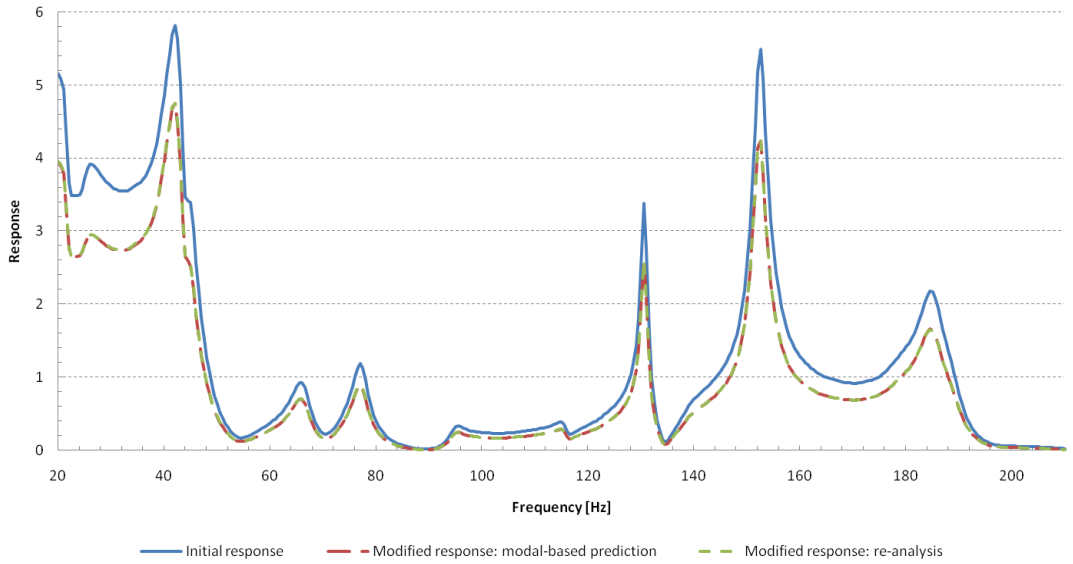

Figure 6: Comparison of the model-based prediction with re-analysis for a parameter modification of 25 % (front-left isolator).

4 Optimization of the Complete Exhaust System

4.1 Goal

As stated above the goal of the optimization will be to bring all the forces in the isolators below the acceptable level, by modifying the structure as little as possible.

In this step of the development project, the geometrical definition of the exhaust system is frozen (size and location of the volumes, layout and hanging points cannot be changed). Changes to the decoupling elements are the only changes that can be considered. The target is now to define the right stiffness values of ball-joints and isolators that will allow reaching the design requirements.

4.2 Parameter Impact Study

There are 18 potential optimization parameters in the FE-model: 3 translational and 3 rotational stiffness coefficients of the ball-joint (6), and the 3 translational stiffness coefficients of the 4 isolators (12). However, it is not certain that all those 18 parameters have a sufficient impact on the forces transmitted through the isolators.

The effect of the optimization parameters on the transmitted forces was evaluated by modifying the parameters one by one, using a parameter modification of 25%, and verifying the correlation between the harmonic responses of the initial and perturbed model. The correlations between the harmonic responses are quantified by the signature assurance criterion (SAC) and amplitude difference (AD) values between the amplitudes of the two considered response functions. The SAC and AD value between two responses are defined as [5]:

$$SAC = \frac{\left| HR(\omega)_1^T \; HR(\omega)_2 \right|^2}{\left(HR(\omega)_1^T \; HR(\omega)_1 \right)\left(HR(\omega)_2^T \; HR(\omega)_2 \right)} \tag{10}$$

$$AD = \frac{\sum_{\omega} HR(\omega)_2 - \sum_{\omega} HR(\omega)_1}{\sum_{\omega} HR(\omega)_1} \tag{11}$$

The SAC value describes the difference in shape between two responses: two responses with a SAC value of 100% have an identical shape; two responses with a SAC value of 0% have an uncorrelated shape. The SAC value only depends on the shape of the functions; it is insensitive to differences in the average amplitude. The AD describes the difference in the average amplitude between two compared functions. Two functions with identical average amplitude have an AD value of 0%.

The SAC and AD values were computed for the transmitted forces in the Z-direction of the four isolators, and this for the 18 potential optimization parameters. Table 4 presents the average and extreme value of the SAC and AD values for the 12 considered response functions.

	Ball-joint					
	K_x	K_y	K_z	H_x	H_y	H_z
Mean SAC	100.0%	100.0%	100.0%	100.0%	**99.1%**	**98.9%**
Min SAC	100.0%	100.0%	100.0%	100.0%	**98.9%**	**97.0%**
Mean AD	0.7%	0.0%	0.1%	0.0%	**1.3%**	**1.2%**
Max AD	0.7%	0.1%	0.2%	0.0%	**2.4%**	**3.0%**

	Isolator front left			Isolator front right		
	K_x	K_y	K_z	K_x	K_y	K_z
Mean SAC	100.0%	100.0%	**99.8%**	100.0%	100.0%	**99.8%**
Min SAC	100.0%	100.0%	**99.5%**	100.0%	100.0%	**99.7%**
Mean AD	0.0%	0.1%	**7.3%**	0.0%	0.1%	7.5%
Max AD	0.0%	0.1%	**22.3%**	0.0%	0.1%	**21.2%**

	Isolator rear left			Isolator rear right		
	K_x	K_y	K_z	K_x	K_y	K_z
Mean SAC	100.0%	100.0%	**99.9%**	99.9%	100.0%	99.8%
Min SAC	100.0%	100.0%	**99.8%**	99.8%	100.0%	99.5%
Mean AD	0.2%	0.0%	6.8%	2.4%	2.2%	**7.7%**
Max AD	0.4%	0.1%	**22.3%**	0.1%	0.1%	**26.8%**

Table 4: The results of the parameter impact study.

The results presented in Table 4 indicate that the effect of a modification of the three translational stiffness coefficients of the ball-joint on the shape and the amplitude of the considered response functions is insignificant. The translational stiffness coefficients can thus be eliminated from the list of optimization parameters. The effect of the rotational stiffness coefficient H_x of the ball-joint is insignificant as well. However, the rotational stiffness coefficients H_y and H_z appear to have an effect on the shape of the response function. Both H_y and H_z, especially H_y, have an effect on the average amplitude of the transmitted forces.

The stiffness coefficients of the springs have both an effect on the shape and on the average amplitude of the transmitted forces. Note that a modification of the stiffness in a particular direction of an isolator mainly affects the force transmitted in the considered direction of the considered isolator. The effect on the forces transmitted in the other directions, and through the other isolators is limited. Also note that all the forces in the *X*- and *Y*-directions are well below the acceptable limits. Therefore, it does not appear to be useful to consider K_x and K_y of the isolators as independent optimization parameters. Instead, the stiffness of the isolators will be optimized by considering a stiffness scaling factor that modifies K_x, K_y,

and K_z of the isolators in an identical way. To reduce the number of different parts in the final design, the stiffness of the two isolators in the front, and the isolators in the rear are identical.

Table 5 provides an overview of the 4 independent parameters that are retained for the optimization of the exhaust system.

Parameter	Description
H_y	Rotational stiffness of the ball-joint around the local Y-axis
H_z	Rotational stiffness of the ball-joint around the local Z-axis
D_1	Scaling factor of the stiffness of the front isolators
D_2	Scaling factor of the stiffness of the rear isolators

Table 5: The selected optimization parameters.

The parameter impact study also indicated that an increase of the rotational stiffness of the ball-joint decreases the force transmitted though the isolators, while an increase in the isolator stiffness increases the transmitted forces.

4.3 Optimization

The objective function of the optimization problem is defined as the sum of squares of the relative changes of the optimization parameters. The use of this objective function thus results in an optimized model that differs as little as possible from the initial model. The acceptable levels for the forces transmitted through the isolators are added as constraints. Mathematically, the optimization problem is expressed as:

$$\begin{aligned} &\text{Minimize} && f_0 = \sum_{i=1}^{6} \left(\frac{p_i^0 - p_i}{p_i^0} \right)^2 && \\ &\text{Subject to} && g_i = F_i(\omega) - F_a(\omega) \le 0 && \forall i = 1,\ldots 12 \\ & && p_i \ge p_i^{\min} && \forall i = 1,\ldots 4 \\ & && p_i \le p_i^{\max} && \forall i = 1,\ldots 4 \end{aligned} \tag{12}$$

in which p_i^0 and p_i are the reference[1] and current values of the optimization parameter, $F_i(\omega)$ is the transmitted force of the i^{th} response, and $F_a(\omega)$ is the admissible force level as a function of frequency. The side constraints on the optimization parameters represent the feasible range of stiffness values for the ball-joint and isolators.

The optimization is performed with the FEMtools Optimization module using a gradient-based optimizer [6], which requires the gradients of the objective and constraint functions. The evaluation of the gradients of the objective function is straightforward. The gradients of the constraint functions can be computed with a finite difference approach using the harmonic response modification that was introduced in section 3.2.

Since the results obtained using harmonic response modification are only valid for a limited change of the optimization parameters, the optimization is performed using a double iteration loop. The inner iteration loop optimizes the values of the optimization parameter using only the modal-based harmonic response modification technique. The mode shapes are never recomputed in the inner iteration loop. In the inner optimization loop, the modification of the parameter values is limited to 30%.

Once the solution in the inner iteration loop has converged, the inner loop is aborted, and the optimization procedure returns to the outer iteration loop. The outer iteration loop just re-computes the mode shapes based on the current parameter values. Once the new shapes are computed, a new inner iteration loop is

[1] The values of the updated FE-model.

started. In this way, the number of (computationally expensive) mode shape evaluations can be minimized. To overall solution was considered to be converged when the inner iteration loop modified the parameter less than 0.25%. The whole procedure was automated using The FEMtools Script programming language.

The optimization problem was solved using the updated values of H_y and H_z, and the minimal allowed values for K_z. These values were chosen because they provide a feasible design. The values of the parameters were then optimized in order to obtain a model that was as close as possible to the updated model, while respecting the imposed limit on the transmitted forces. Table 6 presents the results obtained.

Parameter	Modification with respect to the updated model
H_y	+ 0.0%
H_z	+ 0.0%
D_1	- 83.0%
D_2	- 82.7%

Table 6: The optimal design.

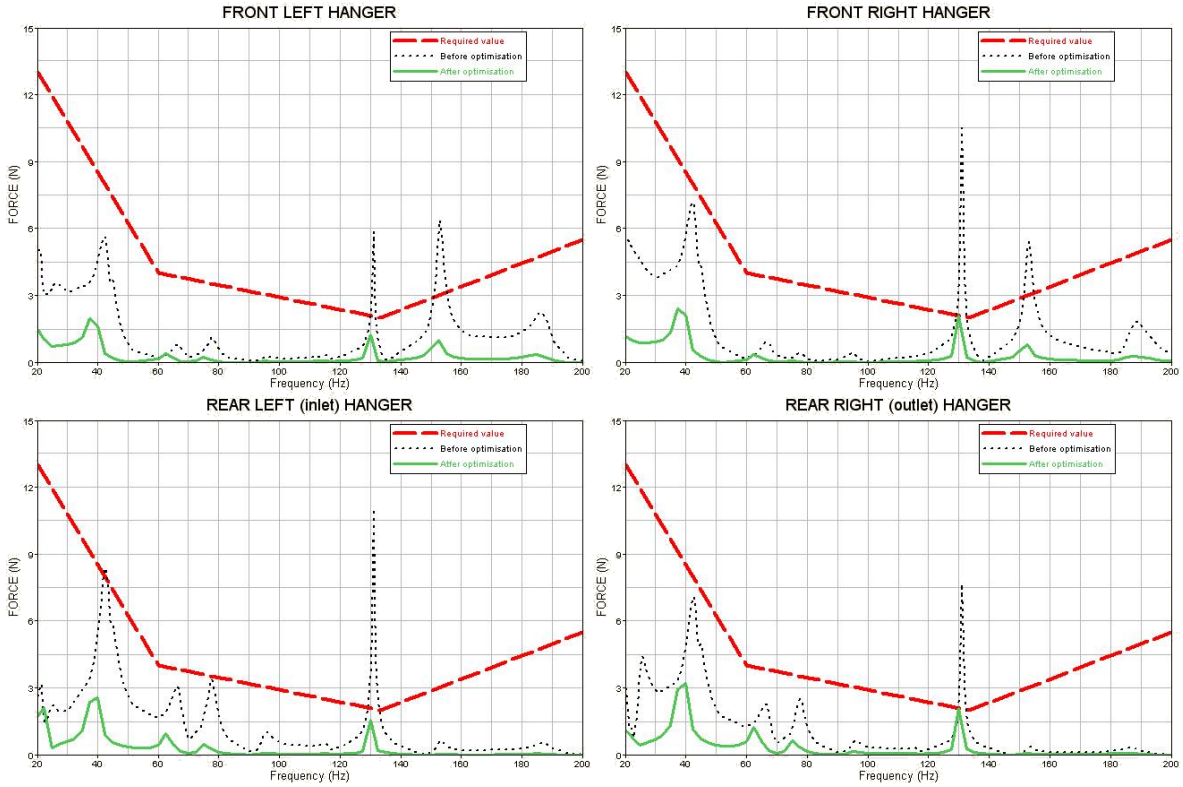

Figure 7: Hanging forces of the optimized model under engine load. The transmitted forces (black) compared to the design specifications (red) in the local *Z*-direction.

The optimization routine did not modify the stiffness of the ball-joint. It thus appears that the cost (deviation from the initial design) for modifying the stiffness of the ball-joint is higher than the benefit (the reduction of the transmitted force). The stiffness of both the front and rear isolators had to be reduced by 83% in order the meet the design specifications.

The optimization problem was also solved without using the upper limit of 30% on the parameter modifications in the inner loop. Solving the problem without considering these bounds provided the same solution, however, now the results converged after only 2 outer iterations instead of 4. The total number of inner iterations was 14 for the first approach and 7 for the second approach. Table 7 provides an

overview of the iteration histories of the two optimization runs. The fact that both optimization results converged to the same solution illustrates the robustness of the obtained solution.

Note that without the use of the modal-based approximation technique it would take about 2 hours to solve the optimization problem, instead of the 13 minutes it took now[2].

Step	Parameter				Iterations	Time [s]	
	H_y	H_z	D_1	D_2		Inner	Outer
Start	0.0%	0.0%	84.0%	92.8%			208.2
1	0.0%	0.0%	83.5%	90.7%	4	194.1	209.3
2	0.0%	0.0%	83.5%	87.8%	4	194.8	209.7
3	0.0%	0.0%	83.2%	84.2%	4	194.7	209.1
4	0.0%	0.0%	83.0%	82.7%	2	129.6	
Result	0.0%	0.0%	83.0%	82.7%	Total		1549.5

(a) The iterations history for the first optimization approach (30% parameter bounds)

Step	Parameter				Iterations		Time [s]
	H_y	H_z	D_1	D_2	H_y	H_z	D_1
Start	0.0%	0.0%	84.0%	92.8%			208.9
1	0.0%	0.0%	82.6%	82.4%	5	232.7	209.5
2	0.0%	0.0%	83.0%	82.7%	2	130.6	
Result	0.0%	0.0%	83.0%	82.7%	Total		781.7

(b) The iterations history for the second optimization approach (no parameter bounds)

Table 7: The iteration histories.

5 Conclusions

This article presented an optimization approach to optimize the harmonic response of industrial-sized FE-models. The presented optimization approach was successfully used to optimize the dynamic performance of a complete exhaust system. The following conclusions can be drawn for the presented case:

1) The modal-based approximation technique appears to be well suited to solve optimization problems like the one presented in this paper. For the considered exhaust system, the use of the modal based-approximation technique reduced the required computation time with a factor of about 10. The benefit of using the modal-based approach will further increase with an increasing number of optimization parameters and model size.
2) The predictive range of the modal-based approximation technique appeared to be larger than initially expected. Therefore, it was not beneficial to limit the parameter changes in the inner iteration loop. For the considered exhaust system, omitting the parameter bounds in the inner iteration loop provided a faster convergence without showing any signs of unstable behavior. Note that the parameters that were selected in the presented test case had a relatively limited effect on the mode shapes. As the modal-based approximation heavily relies on the mode shapes, its predictive capability might go down if the selected optimization parameters have a severe impact on the mode shapes.
3) Until now, the use of mathematical tools allowed to study the dynamic behavior of full exhaust systems under engine loads in early stages of conception. With the methodology presented in this paper, it is possible to go forward, optimizing components from the beginning of the development process. The time spent in trial and error analysis to evaluate the impact of the characteristics of the

[2] All calculations were performed on a standard PC with an Intel dual-core 6600 2.4GHz processor and 4 GB of RAM running Windows Vista 64-bit.

decoupling elements on the exhaust system response is saved. With the presented approach, the process of finding the best compromise between changing the stiffness of the ball-joint and the isolators is automated. It is now possible to identify the most important parameters, and to meet the customer's requirement using the FE model of the complete exhaust system.

Acknowledgements

The authors wish to thank Faurecia Exhaust System Division-R&D Center and Dynamic Design Solutions for offering and supporting the opportunity to write and present this paper.

References

[1] www.femtools.com

[2] Heylen W., Lammens, S., Sas, P. Modal Analysis Theory And Testing, Katholieke Universiteit Leuven, 2007, Leuven, Belgium.

[3] Kundra, K. T. Structural dynamic modifications via models, Sadhana, Vol. 25, Part 3, June 2000, pp. 261-276.

[4] Avitable Peter, Twenty years of structural dynamic modification: A review. S.V. Sound and vibration, vol. 37, n°1, 2003, pp. 14-27.

[5] Grafe H. Model Updating of Large Structural Dynamics Models Using Measured Response Functions. PhD Thesis, Imperial College, October 1998, London, UK.

[6] FEMtools Optimization User's Guide, June 2008.